SANDIA REPORT
SAND99-3190
Unlimited Release
Printed December 1999

Turbulence Radiation Interaction Modeling in Hydrocarbon Pool Fire Simulations

Shawn P. Burns

Prepared by
Sandia National Laboratories
Albuquerque, New Mexico 87185 and Livermore, California 94550

Sandia is a multiprogram laboratory operated by Sandia Corporation, a Lockheed Martin Company, for the United States Department of Energy under Contract DE-AC04-94AL85000.

Sandia National Laboratories

Issued by Sandia National Laboratories, operated for the United States Department of Energy by Sandia Corporation.

Available to DOE and DOE contractors from
Office of Scientific and Technical Information
P.O. Box 62
Oak Ridge, TN 37831

Prices available from (703) 605-6000
Web site: http://www.ntis.gov/ordering.htm

Available to the public from
National Technical Information Service
U.S. Department of Commerce
5285 Port Royal Rd
Springfield, VA 22161

DISCLAIMER

Portions of this document may be illegible in electronic image products. Images are produced from the best available original document.

SAND 99-3190
Unlimited Release
Printed December 1999

Turbulence Radiation Interaction Modeling in Hydrocarbon Pool Fire Simulations

Shawn P. Burns
Engineering Sciences Center
Sandia National Laboratories
P.O. Box 5800
Albuquerque, New Mexico 87185-0835

Abstract

The importance of turbulent fluctuations in temperature and species concentration in thermal radiation transport modeling for combustion applications is well accepted by the radiation transport and combustion communities. A number of experimental and theoretical studies over the last twenty years have shown that fluctuations in the temperature and species concentrations may increase the effective emittance of a turbulent flame by as much as 50% to 300% over the value that would be expected from the mean temperatures and concentrations. With the possibility of such a large effect on the principal mode of heat transfer from a fire, it is extremely important for fire modeling efforts that turbulence radiation interaction be well characterized and possible modeling approaches understood. Toward this end, this report seeks to accomplish three goals. First, the principal turbulence radiation interaction closure terms are defined. Second, an order of magnitude analysis is performed to understand the relative importance of the various closure terms. Finally, the state of the art in turbulence radiation interaction closure modeling is reviewed.

Hydrocarbon pool fire applications are of particular interest in this report and this is the perspective from which this review proceeds. Experimental and theoretical analysis suggests that, for this type of heavily sooting flame, the turbulent radiation interaction effect is dominated by the nonlinear dependence of the Planck function on the temperature. Additional effects due to the correlation between turbulent fluctuations in the absorptivity and temperature may be small relative to the Planck function effect for heavily sooting flames. This observation is drawn from a number of experimental and theoretical discussions. Nevertheless, additional analysis and data is needed to validate this observation for heavily sooting buoyancy dominated plumes.

Acknowledgment

A number of individuals provided their insights and suggestions during the development of this report. The author would like to gratefully acknowledge the contributions of Professor Philip Smith of the University of Utah and Professor Michael Modest of The Pennsylvania State University for their insights regarding the assumed and direct probability density function methods. Dr. Sheldon Tieszen and Dr. Louis Gritzo of Sandia National Laboratories also provided insights into fire phenomenology and Dr. Paul DesJardin of Sandia also provided insight into large eddy simulation methods.

CONTENTS

FIGURES

TABLES

NOMENCLATURE

Special Symbols

$'$	=	Reynolds turbulent fluctuating component.
$''$	=	Favre turbulent fluctuating component.
$\bar{}$	=	Reynolds averaged quantity.
$\tilde{}$	=	Favre averaged quantity.
$\langle\ \rangle$	=	Ensemble averaged quantity

General

a,b	=	Exponents of the general beta probability density function.
Bz	=	Boltzmann number (convection transport / radiation transport).
C	=	Scale constant for the general beta probability density function.
c_p	=	Constant pressure specific heat.
D	=	Diameter.
e_b	=	Planck's black body emission function.
f	=	General mixing variable, usually the mixture fraction.
Fo	=	Fourier number, (heat conduction rate / thermal energy storage rate).
G	=	Scalar flux.
h	=	Enthalpy.
I	=	Intensity.
k	=	Turbulent kinetic energy.
L	=	Length scale.
M_n	=	nth moment of the probability density function.
N	=	Number density.
p	=	Pressure.
P(f;g)	=	Probability density function for f with function shape determined by g.
q	=	Heat flux.

Q	=	Radiative source term.
s	=	Distance along the ordinate direction vector $\hat{s}$.
$\hat{s}$	=	Unit ordinate direction vector.
t	=	Time.
Δt	=	Time step or time averaging period.
T	=	Temperature.
u, v, w	=	Velocity components.
$\mathbf{u}$	=	Velocity vector.
$\mathbf{V}$	=	Ratio of diffusion velocity to scale velocity.
$\mathbf{x}$	=	Position vector.
X	=	Volume fraction.
Y	=	Mass fraction.

Greek

α	=	Flame volume ratio.
γ	=	Thermal diffusivity.
δ	=	Turbulence integral scale, largest turbulent eddy scale.
ε	=	Turbulent dissipation rate.
η	=	Reaction variable.
θ	=	Zenith angle.
κ	=	Turbulent eddy length scale.
λ	=	Radiation wavelength.
μ_a	=	Absorption coefficient.
ν	=	Kinematic viscosity.
π	=	Mixing variable.
ρ	=	Density.
σ	=	Stefan-Boltzmann constant.
ϑ	=	Integrating factor.
ϕ	=	Azimuthal angle, also local stoichiometry.

Subscript

i	=	Chemical species i.
i,j	=	Indicates specific mixing or reaction variables.
r	=	Radiative.
o	=	Scale or reference value.
p	=	Soot or Lagrangian particle.

1.0 INTRODUCTION

The importance of turbulence radiation interaction (TRI) in turbulent combustion applications is by now well accepted in the thermal radiation transport and combustion communities. This observation is supported by experimental studies conducted mostly by Faeth and Gore and their co-workers over the last 13 years for a number of fuels (Kounalakis, et al., 1991, Sivathanu, et al. 1990, Gore and Faeth, 1988, Kounalakis, et al., 1988, Gore, et al., 1987, Gore and Faeth, 1986, Faeth, et al., 1985). This experimental data demonstrates that, depending on the fuel, the radiative emission from a turbulent flame may be as much as 50-300% higher than would be expected based on the mean temperature and absorption coefficient.

Theoretical studies provide additional support for the importance of TRI in combustion applications. Cox (1977) conducted a theoretical analysis of flames traveling in a ceiling layer and suggested that the temperature fluctuations would increase the emission from a turbulent flame by over 100% if the turbulent temperature fluctuation intensities exceeded 41%. Cox also suggested that turbulent fluctuations in the absorption coefficient would provide a further increase in the flame emission but did not elaborate for lack of data. Kabashnikov and Kmit (1979) and Kabashnikov and Myasnikova (1985) also provided a theoretical analysis of the effect of turbulent fluctuations in the temperature and absorption coefficient on thermal radiation. These authors also formalized the thin eddy approximation which is commonly employed in TRI closure models.

In addition to the experimental and theoretical evidence, idealized numerical studies have been used both to demonstrate the effect of TRI as well as to study the effect of different parameters on the overall TRI effect. Soufiani, et al. (1990) examined relatively cool (1000K) turbulent gas flow in a channel without combustion. Nelson (1989a, 1989b) conducted an idealized numerical study of turbulent combustion of carbon monoxide, hydrogen, and methane and concluded that turbulent temperature fluctuations dominated the TRI effect. Mazumder and Modest (1997a) also conducted a numerical analysis of an enclosed methane combustor and concluded that TRI increased the wall heat flux by 40-45% over predictions based on the mean temperature and absorption coefficient.

The work of these and other authors suggests that the magnitude of the TRI effect may be influenced by a number of parameters. For example, the effect of soot concentration was considered by Gore and Faeth (1988) as well as Coppalle and Joyeux (1994). The effect of buoyancy was also considered by Coppalle and Joyeux and Nelson (1989a) noted that scalar fluctuations in buoyant flows may be much larger than in momentum dominated flows. Recognizing these various effects, the remainder of this report will nevertheless remain focused on the effects of TRI in large scale hydrocarbon pool fire applications.

1.1 Large Scale Hydrocarbon Pool Fire Environment

Before proceeding to a detailed discussion of TRI, it is important to describe the perspective from which this discussion proceeds and thereby provide the context for much of the theoretical development presented in the remainder of this report. The principal application of interest in this report is large scale, heavily sooting, hydrocarbon pool fires. This application is relevant to a

number of areas including transportation safety analysis and accident scenarios involving liquid hydrocarbon fuel fires.

An example of a typical hydrocarbon pool fire in a quiescent environment is given in Figure 1.1[1]. The combustion environment shown may be characterized in general terms as a turbulent diffusion flame. Heat from the fire plume causes the liquid fuel to vaporize creating a fuel rich core. Combustion occurs around the periphery of the fire where the fuel vapor and air come into contact. Buoyancy induced flow then gives rise to large scale turbulent motion which has a well characterized vortex shedding or "puffing" frequency (Bejan, 1991). Pyrolosis of the fuel vapor also generates high concentrations of soot particles which tend to form into aggregates as shown in the inset of Figure 1.1.

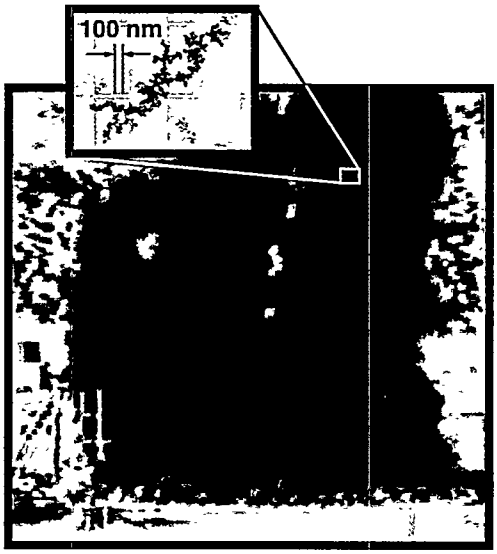

TABLE 1.1 - Jet fuel pool fire characteristics.

Quantity	Value
Length scale, L_o (pool diameter)	10 m
Temperature scale, T_o	1500 K
Time scale, t_o (puffing frequency)[a]	2 s
Velocity scale, v_o	5 m/s
Pressure scale, p_o	1 atm
Enthalpy scale, h_o (C_9H_{20} enthalpy of formation)	1.8 MJ/kg

a. Bejan, 1991

FIGURE 1.1 - Typical pool fire geometry and characteristic values.

Assuming that the material properties within the plume, e.g., specific heat, thermal conductivity, viscosity, etc., are close to those of air, it is possible to estimate the value of several relevant dimensionless groups using the characteristic values given in Table 1.1. Typically, Mach numbers within the plume will be small, $O(10^{-3})$, allowing flow work terms to be neglected in the conservation of energy equation. The Reynolds number based on the pool diameter and characteristic velocity will be relatively high, $O(10^5)$, and the Boltzmann number (ratio of advection to radiative transport) should be of order one.

1. Graphics courtesy of Louis A. Gritzo, and Jill Williams of department 9116.

Puri (1993, pg. 16-20) provides the appropriate form for the conservation of energy equation for combustion processes. Ignoring flow work and work due to body forces and neglecting the Soret and Dufour effects and further assuming that the mass diffusion fluxes may be described by a single diffusion coefficient, the conservation of energy equation may be written in nondimensional enthalpy form as

$$\frac{D(\rho h)}{Dt} = \frac{\nabla \cdot (\rho\gamma \nabla h)}{RePr} - \frac{1}{Re}\left(\frac{1}{Pr} - \frac{1}{Sc}\right)\nabla \cdot \left[\rho\gamma \sum_k h_k \nabla Y_k\right] - \frac{\nabla \cdot q_r}{Bz}, \tag{1.1}$$

where Re is the Reynolds number, Pr is the Prandtl number, Sc is the Schmidt number, and Bz is the Boltzmann number. Assuming Pr and Sc are $O(10^0)$ and neglecting terms of O(1/Re), then Equation (1.1) shows that the heat transfer within a fire plume is dominated by advection and radiation mechanisms.

Experimental data shows that the radiative emission from the plume is dominated by the soot phase and to a lesser extent by the gas phase, e.g., CO_2, H_2O, fuel vapor, etc. (Modest, 1993, pg. 425). Köylü and Faeth (1992) showed that the diameter of the fundamental soot particles range from 10 to 50 nm for a number of fuels. Modest suggests the range extends from 5 to 80 nm. The dominant radiation wavelength predicted by Wein's displacement law (Siegel and Howell, 1992, pg. 29) for T= 1500 K (cf. Table 1.1) is 1.9 μm. Based on this wavelength, the scattering albedo for spherical particles of this size is given by the Rayleigh scattering limit (Siegel and Howell, pg. 577-581) to be $O(D_p^3/\lambda^3)=O(10^{-7})$ to $O(10^{-5})$. Thus, scattering from soot particles may be neglected to a good approximation. Additionally, since the soot phase emits radiation in a continuous spectrum and the absorption coefficient from Rayleigh theory is inversely proportional to wavelength, a wavelength mean absorption coefficient may be used with the assumption of gray transport.

For these reasons, the radiative transport within the plume is governed by the gray, nonscattering form of the Boltzmann transport equation. Additionally, since the radiative transport occurs on a time scale much smaller than the fastest chemical reaction (Mazumder and Modest, 1997a) the transient term may also be neglected resulting in the steady Boltzmann transport equation

$$\hat{s} \cdot \nabla I(x, \hat{s}) + \mu_a(x) I(x, \hat{s}) = \mu_a(x) \frac{\sigma T^4(x)}{\pi}. \tag{1.2}$$

It should be noted that the radiative properties of agglomerated soot particles such as shown in the inset in Figure 1.1 may have significantly different scattering properties than those of spherical particles (Köylü and Faeth, 1996). Nevertheless, for the purposes of this report, the radiative transport within the plume shown in Figure 1.1 is assumed to be governed by the steady state Boltzmann equation for a gray, nonscattering, absorbing and emitting medium.

1.2 Overview

This report has three principal objectives: to characterize principal TRI closure terms; to evaluate the order of magnitude contribution of each of the TRI closure terms to the overall effect; and to assess the current state of the art in TRI closure modeling. Each of these goals is addressed in turn in the succeeding chapters of this report. Chapter 2 derives each of the TRI closure terms arising from the conservation of energy equation and the Boltzmann transport equation. Chapter 3 provides an order of magnitude analysis for each of the closure terms for the hydrocarbon pool fire environment described in the previous section. Chapter 4 reviews the numerical models described in the open literature which have been used to provide TRI closure for combustion applications. Finally, Chapter 5 summarizes the principal observations made in the earlier chapters and makes recommendations for implementing TRI closure models for the hydrocarbon pool fire environment.

It should be recognized that this report does not go into the details of specific turbulent mixing and reaction models. Where necessary, specific reaction and mixing models are described in general terms and relevant citations listed. The literature concerning reaction and mixing models is quite extensive, however, and the validity of various models under different conditions is a subject unto itself. This report describes the various numerical implementations referenced in the open literature to achieve TRI closure but leaves off where the turbulent reaction and mixing model begins.

2.0 DEFINITION

This chapter provides a definition of the principal terms involved in the turbulence radiation interaction (TRI) closure. In general, TRI arises from the filtering procedure used to obtain the mean conservation of energy equation. Although the spatial filtering employed in large eddy simulations (LES) also gives rise to TRI effects, the majority of the open literature approaches TRI from the standpoint of time averaging. Therefore, this will be the standpoint adopted in this report. Section 2.1 provides a brief review of the averaging procedure used in Reynolds and Favre time averaging. Section 2.2 and Section 2.3 then discuss the time averaged conservation of energy and Boltzmann transport equations and describe the resulting TRI terms. Section 2.4 provides some discussion of LES modeling and Section 2.5 summarizes the principal TRI terms arising from time averaging.

2.1 Time Averaging

The time averaging procedure assumes that the principal flow quantities, e.g., velocity components, temperature, species concentration, etc., are comprised of a steady component and a turbulent component which varies rapidly in time (Wilcox, 1998, pp. 31-32). Thus, the instantaneous temperature at location **x** and time t is given by

$$T(x,t) = \overline{T}(x) + T'(x,t). \tag{2.1}$$

The mean temperature is then given by the time average

$$\overline{T}(x) = \lim_{\Delta t \to \infty} \left(\frac{1}{\Delta t}\right) \int_{t_o}^{t_o + \Delta t} T(x,t)dt. \tag{2.2}$$

Substituting Equation (2.1) into Equation (2.2) results in the identities

$$\overline{T}'(x) = 0, \tag{2.3}$$

and

$$\overline{\overline{T}}(x) = \overline{T}(x). \tag{2.4}$$

In the strictest terms, Equation (2.1) and Equation (2.2) apply only to stationary turbulence in which the mean flow does not vary with time (Wilcox, 1998, pg. 32). Nevertheless, transient mean flows are often considered as well in turbulent applications. Time averaging may still be applied in this case provided that there is a clear separation in time scales between the turbulent fluctuations and variations in the mean flow. In this case

$$\overline{T}(x,t) = \underset{\tau_m \gg \Delta t \gg \tau_t}{\text{Lim}} \left(\frac{1}{\Delta t}\right) \int_{t_o}^{t_o+\Delta t} T(x,t)dt, \tag{2.5}$$

where τ_t is the time scale of the turbulent fluctuations and τ_m is the mean flow time scale (Wilcox, pg. 33). For the remainder of this report it will be assumed that the mean flow is steady so that Equation (2.2) is the appropriate form for the mean temperature.

Favre averaging is an alternative to the Reynolds averaging described above which is often used in turbulent reacting flow problems since it simplifies the governing time averaged equations. Typically, the Favre averaged temperature is represented by an expression similar to Equation (2.1)

$$T(x,t) = \tilde{T}(x) + T''(x,t). \tag{2.6}$$

The Favre averaged temperature is related to the Reynolds averaged temperature by the expression (Smoot and Smith, 1985, pg. 279)

$$\tilde{T}(x) = \frac{\overline{\rho(x)T(x)}}{\bar{\rho}(x)} = \overline{T}(x)\left(1 + \frac{\overline{\rho'(x)T'(x)}}{\bar{\rho}(x)\overline{T}(x)}\right). \tag{2.7}$$

Throughout the remainder of this report both Reynolds and Favre time averaging will be referred to loosely as "time averaged" quantities. Flow quantities will be referred to explicitly as either Reynolds averaged or Favre averaged in cases where the precise definition is required for understanding.

2.1.1 Probability Density Function Description

An alternative description of the mean of a turbulent fluctuating property is provided by a statistical probability density function (pdf) (Pope, 1985)

$$\overline{T}(x) = \int_0^\infty T(x)P(T(x))dT(x) \ . \tag{2.8}$$

where the pdf function P(T(x)) is the probability that the temperature at location x lies between T and T+dT. In general, the pdf function varies from location to location in the flow.

The Favre averaged temperature may also be expressed in terms of a pdf

$$\tilde{T}(x) = \int_{-\infty}^{\infty} T(x)\tilde{P}(T(x))dT(x), \tag{2.9}$$

where the Favre averaged pdf is given by (Smoot and Smith, 1985, page 280)

$$\tilde{P}(T(x)) = \frac{\int_0^\infty \rho(x) P(\rho(x), T(x)) d\rho(x)}{\bar{\rho}(x)} . \qquad (2.10)$$

$P(\rho(x), T(x))$ is the joint pdf of density and temperature, i.e., the probability that the density and temperature lay within the bounds $\rho(x)$, $T(x)$ and $\rho(x)+d\rho(x)$, $T(x)+dT(x)$.

2.2 Time Averaged Energy Equation

The time averaged energy equation is obtained by substituting expressions similar to Equation (2.1) or Equation (2.6) into the conservation of energy equation (Equation (1.1)) for the enthalpy, velocity, species concentration, etc., and then time averaging the result. For the sake of brevity, the details of this procedure are not reproduced here. Rather, attention is directed to the divergence of the radiative flux term on the right hand side of Equation (1.1). The text by Smoot and Smith (1985, page 241) provide the full time averaged conservation of energy equation.

The divergence of the radiative heat flux vector which appears on the right hand side of Equation (1.1) represents the difference in the emitted and incident radiative energy (Siegel and Howell, 1992, pg. 699, Modest, 1993, pg. 314)

$$\nabla \cdot q_r(x) = \int_0^\infty \nabla \cdot q_r(\lambda, x) d\lambda = \int_0^\infty \mu_a(\lambda, x)[4e_b(\lambda, T(x)) - G(\lambda, x)] d\lambda , \qquad (2.11)$$

where $\mu_a(\lambda,x)$ is the absorption coefficient at location x and wavelength λ. The scalar flux $G(\lambda,x)$ represents the incident radiative energy at the location x and $e_b(\lambda,x)$ is the black body emissive power, given by the Planck distribution (Siegel and Howell, 1992, page 22), which represents the radiative emission from location x. If the absorption coefficient and scalar flux do not vary with wavelength, then the wavelength integral in Equation (2.11) may be completed resulting in the equivalent gray (nonspectral) relation

$$\nabla \cdot q_r(x) = \mu_a(x)[4\sigma T^4(x) - G(x)] , \qquad (2.12)$$

where σ is the Stefan-Boltzmann constant. Equation (2.12) explicitly shows the highly nonlinear dependence of the local emissive power on the local temperature.

Since the absorption coefficient is a strong function of soot and gaseous species concentrations, as well as temperature, turbulent fluctuations in these quantities give rise to turbulent fluctuations in the absorption coefficient. The Planck function is also a highly nonlinear function of the temperature such that turbulent fluctuations in the temperature give rise to much larger variations in the black body emissive power.

Consider expanding the Planck function in a Taylor series about the mean temperature given in Equation (2.1) to obtain

$$e_b(\lambda, T) = \sum_{n=0}^{\infty} \frac{T'^n}{n!} \frac{d^n}{dT^n} e_b(\lambda, T)\Big|_{\overline{T}} \quad . \tag{2.13}$$

Time averaging Equation (2.13) results in an expression for the time averaged emissive power

$$\overline{e_b}(\lambda, T) = \sum_{n=0}^{\infty} \frac{\overline{T'^n}}{n!} \frac{d^n}{dT^n} e_b(\lambda, T)\Big|_{\overline{T}} \neq e_b(\lambda, \overline{T}) \quad . \tag{2.14}$$

The final inequality in Equation (2.14) holds except for the special case of zero temperature fluctuation, i.e., no turbulence. The fluctuating component of the emissive power is given by subtracting Equation (2.14) from Equation (2.13)

$$e_b'(\lambda, T) = \sum_{n=0}^{\infty} \frac{[T'^n - \overline{T'^n}]}{n!} \frac{d^n}{dT^n} e_b(\lambda, T)\Big|_{\overline{T}} \quad . \tag{2.15}$$

The explicit dependence of the temperature on the location x has been dropped in Equation (2.13) through Equation (2.15) for clarity. Integrating Equation (2.14) and Equation (2.15) over all wavelengths results in the expressions

$$\overline{T^4}(x) = \overline{T}^4(x)\left\{1 + 6\frac{\overline{T'^2}(x)}{\overline{T}^2(x)} + 4\frac{\overline{T'^3}(x)}{\overline{T}^3(x)} + \frac{\overline{T'^4}(x)}{\overline{T}^4(x)}\right\}, \tag{2.16}$$

and

$$[T^4(x)]' = \overline{T}^4(x)\left\{4\frac{T'(x)}{\overline{T}(x)} + 6\frac{T'^2(x)}{\overline{T}^2(x)} + 4\frac{T'^3(x)}{\overline{T}^3(x)} + \frac{T'^4(x)}{\overline{T}^4(x)}\right\} + \overline{T}^4(x) - \overline{T^4}(x). \tag{2.17}$$

The time averaged radiative flux divergence (Equation (2.11)) may be written in terms of the mean Planck function as follows

$$\overline{\nabla \cdot q_r}(\lambda, x) = 4\overline{\mu_a}(\lambda, x)e_b(\lambda, \overline{T}(x))\left[\frac{\overline{e_b}(\lambda, T(x))}{e_b(\lambda, \overline{T}(x))} + \frac{\overline{\mu_a'(\lambda, x)e_b'(\lambda, T(x))}}{\overline{\mu_a}(\lambda, x)e_b(\lambda, \overline{T}(x))}\right] - \tag{2.18}$$
$$\overline{\mu_a}(\lambda, x)\overline{G}(\lambda, x) - \overline{\mu_a'(\lambda, x)G'(\lambda, x)}$$

The first term in the square brackets on the right hand side of Equation (2.18) represents the effect of turbulent temperature fluctuations alone while the second term represents the correlation between fluctuations in the absorption coefficient and the temperature. The last term on the right hand side also results from turbulent fluctuations in the absorption coefficient and the scalar flux. It is clear from the form of Equation (2.18) that the radiative flux divergence term for a turbulent flow is very different than the form obtained based on the mean temperature and absorption coefficient.

2.2.1 Time Averaged Scalar Flux

The scalar flux term appearing in Equation (2.11) represents the integral of the incident spectral radiative intensity at a given point over all solid angles (Modest, 1993, pg. 314)

$$G(\lambda, x) = \int_0^{2\pi} \int_0^{\pi} I(\lambda, x, \hat{s}) \sin\theta \, d\theta \, d\varphi, \tag{2.19}$$

where $I(\lambda, x, \hat{s})$ is the spectral radiative intensity at location **x** corresponding to the direction given by the unit vector $\hat{s}$ as shown in Figure 2.1

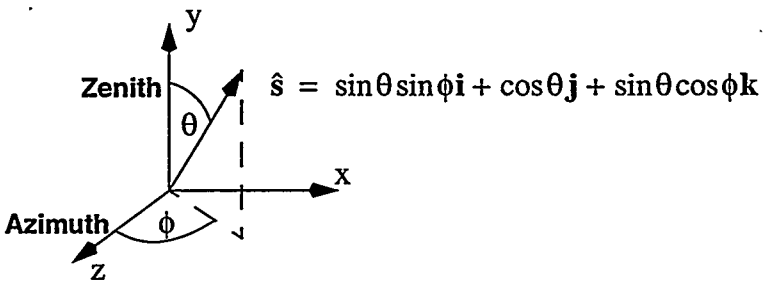

FIGURE 2.1 - Zenith and azimuthal angles defining the unit direction vector.

From Equation (2.19) the mean and fluctuating components of the scalar flux (cf. Equation (2.1)) may be directly related to the mean and fluctuating components of the incident intensity

$$\overline{G}(\lambda, x) = \int_0^{2\pi} \int_0^{\pi} \bar{I}(\lambda, x, \hat{s}) \sin\theta \, d\theta \, d\varphi, \tag{2.20}$$

$$G'(\lambda, x) = \int_0^{2\pi} \int_0^{\pi} I'(\lambda, x, \hat{s}) \sin\theta \, d\theta \, d\varphi. \tag{2.21}$$

The mean and fluctuating components of the radiative intensity must be obtained from the nongray form of the Boltzmann radiative transport equation (cf. Equation (1.2))

$$\hat{s} \cdot \nabla I(\lambda, x, \hat{s}) + \mu_a(\lambda, x) I(\lambda, x, \hat{s}) = \mu_a(\lambda, x) \frac{e_b(\lambda, T(x))}{\pi} . \tag{2.22}$$

2.3 Time Averaged Boltzmann Transport

As described previously (cf. Section 1.1) the radiative transport for the application of interest in this report is assumed to be governed by the Boltzmann transport equation for steady, nonscattering radiative transport. The assumption of gray (no wavelength dependence) transport will be relaxed to be consistent with the development in the previous section. Under these conditions the Boltzmann radiative transport equation may be written as

$$\hat{s} \cdot \nabla I(\lambda, x, \hat{s}) + \mu_a(\lambda, x) I(\lambda, x, \hat{s}) = \mu_a(\lambda, x) \frac{e_b(\lambda, T(x))}{\pi} . \tag{2.23}$$

As before, the absorption coefficient, temperature, and, in this case, the intensity, are assumed to have a steady and turbulent fluctuating component. Substituting these quantities into Equation (2.23) and time averaging results in an equation for the mean intensity

$$\begin{aligned} &\hat{s} \cdot \nabla \bar{I}(\lambda, x, \hat{s}) + \overline{\mu_a}(\lambda, x) \bar{I}(\lambda, x, \hat{s}) + \overline{\mu_a'(\lambda, x) I'(\lambda, x, \hat{s})} = \\ &\overline{\mu_a}(\lambda, x) e_b(\lambda, \bar{T}(x)) \left[\frac{\overline{e_b}(\lambda, T(x))}{e_b(\lambda, \bar{T}(x))} + \frac{\overline{\mu_a'(\lambda, x) e_b'(\lambda, T(x))}}{\overline{\mu_a}(\lambda, x) e_b(\lambda, \bar{T}(x))} \right] . \end{aligned} \tag{2.24}$$

The terms appearing within the bracket on the right hand side of Equation (2.24) are identical to the bracketed terms on the right hand side of Equation (2.18). In addition to the turbulent correlation terms appearing in Equation (2.18), however, Equation (2.24) also includes an absorptivity-intensity correlation term which is the last term shown on the left hand side of Equation (2.24).

2.4 Large Eddy Simulation

Although the remainder of this report will be devoted to time averaging, it is useful to consider the TRI terms which arise in a LES formulation. One of the implications of the spatial filtering used in an LES formulation is that the mean of the mean is no longer equal to the mean (cf. Equation (2.4)). As a result, the cross correlation terms are no longer zero and the radiative flux divergence term shown in Equation (2.18) becomes

$$\begin{aligned} \overline{\nabla \cdot q_r} &= \overline{\mu_a}[4 e_b(\bar{T}) - \bar{G}] + \\ &4[\overline{\overline{\mu_a} e_b}(T) - \overline{\mu_a} e_b(\bar{T}) + \overline{\mu_a} e_b'(T)] + 4[\overline{\mu_a' e_b'}(T) - \overline{\mu_a' e_b}(T)] - \\ &[\overline{\overline{\mu_a} \bar{G}} - \overline{\mu_a} \bar{G}] - [\overline{\overline{\mu_a} G'} - \overline{\mu_a' \bar{G}}] - \overline{\mu_a' G'} , \end{aligned} \tag{2.25}$$

where the dependence of each term on the location, wavelength, and time has been omitted for clarity. The first bracketed term on the right hand side of Equation (2.25) represents the flux divergence based on the mean temperature, absorption coefficient, and radiation field. Drawing parallels with Equation (2.18), the second and third bracketed terms on the right hand side of Equation (2.25) represent the effect of temperature fluctuations and absorptivity-temperature fluctuations respectively. The final three terms on the right hand side of Equation (2.25) represent the effect of the absorptivity-scalar flux fluctuations.

All of the terms on the second and third line of Equation (2.25) require modeling in an LES simulation. In addition, spatial filtering of the Boltzmann equation also generates terms equivalent to the absorptivity-intensity correlation term in Equation (2.24)

$$[\overline{\overline{\mu_a}\bar{I}} - \overline{\mu_a}\bar{I}] + [\overline{\overline{\mu_a}I'} - \overline{\mu_a'\bar{I}}] + \overline{\mu_a'I'}. \tag{2.26}$$

The terms shown in Equation (2.25) and Equation (2.5) define the TRI closure problem in an LES simulation.

2.5 Summary

The objective of this chapter has been to describe the mean field closure terms which arise from the time averaged conservation of energy and Boltzmann radiative transport equations. Equation (2.18) and Equation (2.24) show that there are four principal terms which require some form of modeling: the temperature self correlation term

$$\frac{\overline{e_b(\lambda, T(x))}}{e_b(\lambda, \bar{T}(x))}; \tag{2.27}$$

the absorptivity-temperature correlation term

$$\frac{\overline{\mu_a'(\lambda, x)e_b'(\lambda, T(x))}}{\overline{\mu_a}(\lambda, x)e_b(\lambda, \bar{T}(x))}; \tag{2.28}$$

the absorptivity-intensity correlation term

$$\overline{\mu_a'(\lambda, x)I'(\lambda, x, \hat{s})}; \tag{2.29}$$

and, finally, the absorptivity-scalar flux correlation term

$$\overline{\mu_a'(\lambda, x)G'(\lambda, x)}. \tag{2.30}$$

Each of these terms approaches zero as the turbulence level decreases with the exception of the temperature self correlation term which approaches unity. An order of magnitude estimate for each of these closure terms for heavily sooting hydrocarbon pool fires will be presented in the next chapter.

3.0 ORDER OF MAGNITUDE ANALYSIS

In the previous chapter four terms were identified which arise from the time averaged conservation of energy and Boltzmann radiative transport equations. These terms represent the mean field closure problem for turbulence radiation interaction (TRI). In this chapter, an order of magnitude estimate is made for each of these TRI closure terms for the heavily sooting hydrocarbon pool fire application of interest in this report. Each of the TRI closure terms are analyzed in the succeeding sections of this report using data from the open literature and numerical and analytical techniques.

3.1 Absorptivity-Intensity Correlation

One of the most common approximations made in the open literature for TRI is the thin eddy approximation as described by Kabashnikov and Myasnikova (1985). Kabashnikov suggested that if the mean free path for radiation is much larger than the turbulence length scale, κ, then the absorptivity-intensity correlation may be neglected. The rationae behind this assumption is that the instantaneous local intensity at a point **x** is formed over a path traversing several turbulent eddies. Therefore, the local intensity fluctuations are weakly correlated to the local absorptivity fluctuations.

To describe the thin eddy approximation further, consider the instantaneous Boltzmann radiative transport equation

$$\hat{s} \cdot \nabla I(x, \hat{s}) + \mu_a(x) I(x, \hat{s}) = Q(x), \tag{3.1}$$

where gray transport has been assumed and the radiative source term has been lumped into a single value Q(**x**). The solution to Equation (3.1) depends on an integrating factor given by

$$\vartheta(s) = \exp\{\int \mu_a(s) ds\}, \tag{3.2}$$

where s is measured along the ordinate direction given by the unit vector $\hat{s}$. The corresponding solution to Equation (3.1) is then

$$I(s) = \frac{1}{\vartheta(s)}\{\int \vartheta(s) Q(s) ds + c\}. \tag{3.3}$$

Expressing Equation (3.2) in terms of the mean and turbulent fluctuating absorptivity yields

$$\vartheta(s) = \exp\{\int (\overline{\mu_a}(s) + \mu_a'(s)) ds\}. \tag{3.4}$$

Assuming that the thin eddy approximation is true and neglecting the absorptivity-intensity correlation the time averaged Boltzmann equation may be written

$$\hat{s} \cdot \nabla \bar{I}(x, \hat{s}) + \overline{\mu_a}(x)\bar{I}(x, \hat{s}) = \bar{Q}(x). \tag{3.5}$$

The integration factor corresponding to Equation (3.5) is then

$$\bar{\vartheta}(s) = \exp\{\int \overline{\mu_a}(s)ds\}. \tag{3.6}$$

By comparing Equation (3.2) and Equation (3.6) it becomes clear that the thin eddy approximation implies that

$$\overline{\int \mu_a'(s)ds} = 0. \tag{3.7}$$

Kabashnikov and Myasnikova (1985) provide several conditions for the validity of the thin eddy approximation. In general however, the thin eddy approximation depends on the assumption that the optical thickness of the turbulent eddies is small

$$\mu_a \kappa \ll 1, \tag{3.8}$$

where κ is the turbulent eddy length scale. Krebs, et al. (1996) suggest that an eddy optical thickness limit of less than 0.3 is sufficient to meet this criteria for turbulent combustion of propane in air.

Gritzo, et al., (1998) measured extinction coefficients within a large hydrocarbon pool fire on the order of 10 m^{-1}. On this basis, and using the optically thin limit suggested by Krebs, et al. (1996), the thin eddy approximation would be valid for turbulent eddies of up to 3 cm for large scale hydrocarbon pool fires. An order of magnitude analysis (cf. Appendix A) shows that the Kolmogorov length scale for the smallest turbulent eddies in the pool fire shown in Figure 1.1 is on the order of 10^{-3} to 10^{-2} cm which is well below this limit.

3.2 Absorptivity-Scalar Flux Correlation

Similar arguments may be applied to the intensity-scalar flux correlation as were applied to the absorptivity-intensity correlation. As with the latter term, for cases in which the turbulent eddies are optically thin, the scalar flux at a given location, **x**, depends on the conditions at surrounding points rather than the local conditions. Therefore it may be reasonable to neglect this correlation term for the case of optically thin eddies. This observation was also made by Mazumder and Modest (1997a).

3.3 Temperature Self Correlation

Gray radiative transport will be assumed to illustrate the effect of the temperature self correlation term given by Equation (2.27). For gray radiative transport, the temperature self correlation term is given by Equation (2.16)

$$\frac{\overline{T^4}(x)}{\overline{T}^4(x)} = 1 + 6\frac{\overline{T'^2}(x)}{\overline{T}^2(x)} + 4\frac{\overline{T'^3}(x)}{\overline{T}^3(x)} + \frac{\overline{T'^4}(x)}{\overline{T}^4(x)}. \tag{3.9}$$

It is also convenient for this analysis to represent the temperature fluctuations in terms of a probability density function (pdf) as in Equation (2.8). By adopting an appropriate scaling, the instantaneous temperature may be expressed in terms of its mean value, the standard deviation of the turbulent fluctuations and a dummy variable $0 \le f \le 1$

$$T(f) = \overline{T} + \sqrt{\frac{\overline{T'^2}}{M_2}}(f - \overline{f}), \tag{3.10}$$

where

$$\overline{T} = \int_0^1 T(f)P(f)df, \tag{3.10a}$$

$$\overline{f} = \int_0^1 fP(f)df, \tag{3.10b}$$

and

$$M_n = \int_0^1 (f - \overline{f})^n P(f)df. \tag{3.10c}$$

Through some algebra, the moments of the turbulent temperature fluctuations shown in Equation (3.9) may be expressed in terms of the moments of the pdf given by Equation (3.10c)

$$\frac{\overline{T'^n}(x)}{\overline{T}^n(x)} = \left\{\frac{\sqrt{\overline{T'^2}(x)}}{\overline{T}(x)}\right\}^n \frac{M_n}{M_2^{n/2}}. \tag{3.11}$$

The purpose of this exercise is to show that the gray temperature self correlation term shown in Equation (3.9) may be represented entirely by the characteristics of the pdf function P(f). If it were possible to determine the exact analytical form of the pdf then it would be possible to evaluate the higher moments of the turbulent temperature fluctuations given by Equation (3.11) and evaluate Equation (3.9) directly.

Several authors have presented statistical data for the temperature fluctuations within flames. Krebs, et al. (1996) considered an enclosed propane-air diffusion flame, Coppalle and Joyeux

(1994) considered unconstrained diffusion flames of pure ethelyne in still air. Gore, et al. (1992) and Gritzo, et al. (1998) both considered unconstrained combustion of more heavily sooting fuels in air including acetylene and aviation fuel. All of these authors show that while the pdf of the temperature fluctuation takes a generally Gaussian distribution at many locations in the fire, distinct deviations from a purely Gaussian profile may also be seen.

Krebs, et al. (1996) and Coppalle and Joyeux (1994) suggest that the temperature pdf may be skewed toward higher temperatures within the combustion zone on the centerline but approaches a more Gaussian distribution higher in the flame. The data shown by Coppalle and Joyeux suggests that this skewing in the temperature fluctuation pdf might decrease as the inlet Reynolds number decreases and buoyancy effects become more pronounced. In contrast, the data provided by Gore, et al. (1992) suggests a consistent shift to colder temperatures in the temperature pdf along the fire centerline for the heavily sooting acetylene flame. This cold shift is also reflected in the data provided by Gritzo, et al. (1998). Krebs, et al. also show that the temperature pdf takes on a distinctly bimodal form within the reacting shear layer where intermittency between the cool oxidizer stream and hot combustion products is more pronounced.

While the temperature pdf data presented by these authors is too sparse to draw any general conclusions, they do serve to provide some idea of what types of temperature pdf shapes are seen experimentally. Table 3.1 summarizes the general temperature fluctuation pdf shapes described by the above authors.

TABLE 3.1 - Experimentally observed temperature fluctuation pdfs.

Location	General pdf Shape
Reaction zone centerline	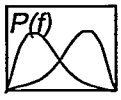
Reacting shear layer	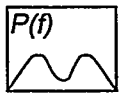
Centerline (outside reaction zone)	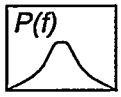

3.3.1 Beta Probability Density Function

A numerical experiment is conducted here in an attempt to evaluate the magnitude of the temperature self correlation term. For the purposes of this experiment the beta function is chosen to represent the pdf of the temperature fluctuations (Puri, 1993). The general form of the beta function pdf is given by

$$P(f) = Cf^{a-1}(1-f)^{b-1}, \tag{3.12}$$

where

$$C = \left[\int_0^1 f^{a-1}(1-f)^{b-1}df\right]^{-1}. \qquad (3.12a)$$

By adjusting the exponents a and b in Equation (3.12) it is possible to generate a number of pdf shapes which approximate the shapes shown in Table 3.1. Seven cases where selected for the purposes of this experiment as shown in Table 3.2. While the beta function pdfs shown in Table 3.2. do not provide an exact match to the experimental data, it is reasonable to expect that the experimental pdf shapes shown in Table 3.1 lay within the envelope described by the seven pdf shapes shown in Table 3.2. Furthermore, it will become clear that the temperature self correlation term is relatively insensitive to the particulars of the shape of the temperature fluctuation pdf.

TABLE 3.2 - Beta pdf functions used to approximate experimental data.

Case	a	b	C	$\bar{f}$	Shape
1	1/2	1/2	$1/\pi$	1/2	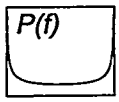
2	1	1	1	1/2	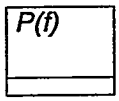
3	5	5	630	1/2	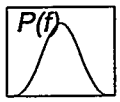
4	2	5	30	2/7	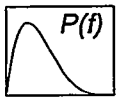
5	5	2	30	5/7	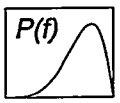
6	1	20	20	1/21	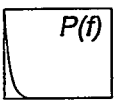
7	20	1	20	20/21	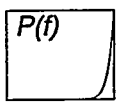

The moments of each of the pdf functions shown in Table 3.1 may now be calculated (cf. Equation (3.10c)) and the variation of the temperature self correlation with the intensity of the temperature fluctuations calculated from Equation (3.11). Figure 3.1 shows the variation of the temperature self correlation term for each of the pdf functions shown in Table 3.2.

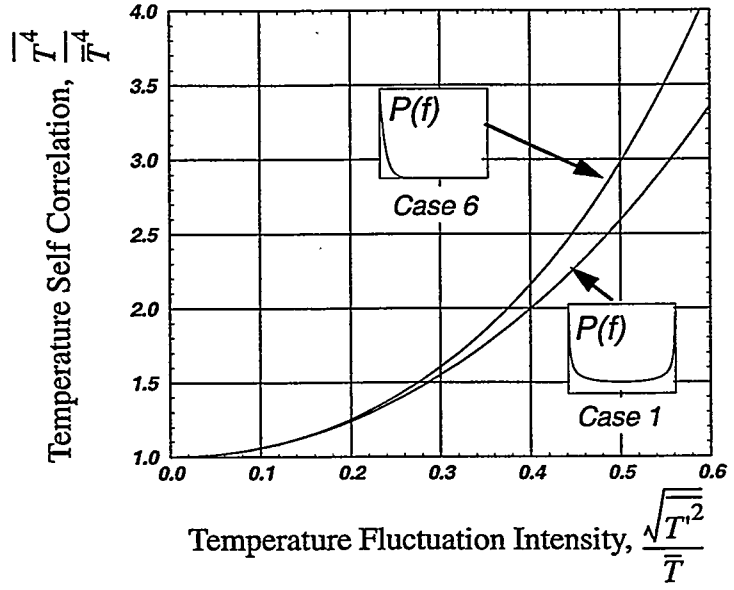

FIGURE 3.1 - Temperature self correlation variation with temperature fluctuation intensity for a number of beta probability density functions.

All of the curves corresponding to the pdfs in Table 3.2 fall between the curves for case 1 and case 6 in Figure 3.1. This is an important observation as it suggests that the magnitude of the temperature self correlation term is relatively insensitive to the shape of the temperature fluctuation pdf. For example, the variation in the temperature self correlation factor shown in Figure 3.1 due to the pdf shape for a temperature fluctuation intensity of 40% is less than 10% of the minimum value. The variation increases to 15% of the minimum value for a fluctuation intensity of 50% and less than 20% of the minimum value at a fluctuation intensity of 60%.

Krebs, et al. (1996) observed temperature fluctuation intensities in the range of 17% to 35%. Similarly, Coppalle and Joyeux (1994) observed temperature fluctuation intensities of approximately 20% which agrees with the work of Cox (1976). Cox also cites theoretical work which suggests that temperature fluctuation intensities may rise as high as 40% to 65% for gas diffusion flames. This theoretical estimate does not appear to be supported by the experimental data, however. Nevertheless, the data shown in Figure 3.1 agrees with Cox's estimate that the effect of the turbulent temperature fluctuations will dominate the mean temperature effects when the temperature fluctuation intensity exceeds approximately 40%. Taking a temperature fluctuation intensity range of 20% to 40% as a reasonable range, Figure 3.1 suggests that the temperature self correlation term may result in an increase of 120% to 200% in the radiative source term in Equation (2.18) and Equation (2.24), i.e., increasing the effective emittance of the flame 1.2 to 2 fold.

3.4 Absorptivity-Temperature Correlation

A number of authors provide simultaneous measurements of the instantaneous temperature and species and soot concentrations at specific locations within nonpremixed flames (Gore and Faeth, 1988, Coppalle and Joyeux, 1994, Krebs, et al. 1996, Gritzo, et al. 1998). Measurements of the species concentrations and temperature at a point in a turbulent reaction zone, however, requires both a high sampling rate and small sample volume to correctly resolve the thin reaction zones, i.e. flame sheets, which characterize this environment. Therefore, the data necessary to evaluate the absorptivity-temperature correlation term (cf. Equation (2.28)) is limited.

Gore and Faeth (1988) provide data for heavily sooting acetylene-air flames. These authors predict that turbulent fluctuations have a strong effect on the soot emission but a negligible effect on soot absorption within the bulk flame. Based on these predictions the authors suggest that turbulence radiation interaction effects in heavily sooting flames are dominated by the temperature self correlation effect. This work of Gore and Faeth is one of the few discussions to explicitly separate the temperature and temperature-absorptivity effect.

Coppalle and Joyeux (1994) also provide data for turbulent temperature-soot concentration fluctuations for a heavily sooting flame. These authors provide optical measurements along the centerline of an ethylene-air jet diffusion flame of both the instantaneous temperature and soot concentration. These authors show that the temperature-soot concentration correlation factor is in the range

$$-0.1 < \frac{\overline{T' X_s'}}{\sqrt{\overline{(T')^2}}\sqrt{\overline{(X_s')^2}}} < 0.4, \tag{3.13}$$

for two Rayleigh numbers. While Equation (3.13) does not provide a precise value for the absorptivity-temperature correlation term, it does suggest that fluctuations in the temperature and absorptivity may be weekly correlated assuming radiative emission is dominated by the soot phase.

Using an idealized numerical model, Nelson (1989a, 1989b) suggests that the nonlinearity of the Planck function, i.e., the temperature self correlation term, dominates the TRI effect for a number of fuels including carbon monoxide, hydrogen, and methane. Nelson further suggests that ignoring absorptivity fluctuations entirely results in errors on the order of 10%. These results agree with the later numerical work performed by Mazumder (1997). Mazumder suggests that including the temperature absorptivity correlation changes the radiative source term by less than 6% of the radiative source based on the mean absorptivity and Planck function evaluated at the mean temperature for heavily sooting flames[1]. These results suggest that numerical simulation of

1. For future reference it should be noted that Equation 2.9 in Mazumder's work (Mazumder, 1997, pg. 15) equates the mean Planck function with the Planck function evaluated at the mean temperature. Personal communication with Mazumder's thesis advisor indicates that this is a typographical error and is not reflected in the subsequent analysis performed by Mazumder.

the absorptivity-temperature self correlation effect is not cost effective for soot dominated applications.

It is reasonable to expect that the contribution of the absorptivity-temperature self correlation term may be very different for nonluminous flames which are not dominated by soot emission (Faeth, et al. 1985). The data provided by Krebs, et al. (1996) suggests that the absorptivity-temperature self correlation effect dominates the temperature self correlation effect. Indeed, spectral intensity predictions based on the mean and the fluctuating temperatures along a line of sight through the flame suggest that there is a negligible temperature self correlation effect. Unfortunately, these authors provide insufficient detail regarding their analysis to determine if this is a valid prediction.[1]

3.5 Summary

An order of magnitude analysis for the four principal TRI closure terms arising from Reynolds time averaging has been conducted using data from the open literature as well as theoretical and numerical predictions. Theoretical analysis suggests that the absorptivity-intensity and absorptivity-scalar flux correlations may be negligible for cases in which the length scale characterizing the turbulent fluctuations is optically small. In contrast, a simple numerical analysis showed that the temperature self correlation, i.e., the nonlinear dependence of the Planck function on the temperature, may readily increase the radiative source term by 100% or more. Furthermore, this same analysis showed that the temperature self correlation is more sensitive to the magnitude of the turbulent temperature fluctuations than the shape of the pdf describing the fluctuations. Finally, only limited data is available to describe the absorptivity-temperature correlation term in general but some limited experimental and numerical data suggests that this effect may be small relative to the temperature self correlation effect for heavily sooting flames.

1. The data provided by Krebs, et al. (1996) shows a 20-30% turbulent temperature fluctuation intensity. The data shown in Figure 3.1 would suggest a significant 25-100% emission increase over that predicted by the mean temperature.

4.0 MODELING APPROACHES

The previous chapters of this report have defined the principal mean field closure terms arising from turbulence radiation interaction (TRI) and have provided an order of magnitude estimate of each term for large scale hydrocarbon pool fire applications. The objective of this chapter is to discuss the state of the art in TRI closure models as described in the open literature. This discussion will employ a probability density function (pdf) description of the turbulent fluctuations in the flow properties. This pdf description provides a convenient framework for describing the various closure modeling approaches and is cast in a more general form in this chapter than in the previous descriptions in Chapter 2 and Chapter 3. The description provided here arises naturally from the work done in chemistry-turbulence interactions (see, for example, Smith and Fletcher, 1988).

In the most general case, the mean radiative source term (cf. the right hand side of Equation (2.24)), $\overline{\mu_a e_b}$ may be given by[1]

$$\overline{\mu_a e_b} = \int_{\eta_j \pi_i} \int \mu_a(\pi_i, \eta_j) e_b(\pi_i, \eta_j) P(\pi_i, \eta_j; \overline{\pi_i}, \overline{\eta_j}, \overline{\pi_i'^2}, \overline{\eta_j'^2}, \ldots) d\pi_i d\eta_j, \tag{4.1}$$

where π_i and η_j are sets of mixing and reaction variables and P(...) is the joint probability density function. The set of mixing variables describe the state of mixing, e.g., mass fractions, while the set of reaction variables describe the extent of the reaction, e.g., enthalpy. The "reaction model", μ_a, $e_b(\pi_i, \eta_j)$, provides the instantaneous flow property at a point given the mixture and reaction variables at that point. The "mixing model" provides the mean flow property and is given by the form of the pdf function P(...). In Equation (4.1), the shape of the pdf function is specified by the value of the mean mixing and reaction variables and the moments of their fluctuations. Although, theoretically, any number of fluctuating moments may be employed to obtain the pdf shape, typically only the mean and the first moment are used.

It is important to note that Equation (4.1) implicitly includes both the absorptivity-temperature correlation and the temperature self correlation. Equation (4.1) does not model either the absorptivity-intensity correlation or the absorptivity-scalar flux correlation. As discussed in Chapter 3 (cf. Section 3.1 (page 27) and Section 3.2 (page 28)) the assumption of optically thin turbulent eddies allows both of these terms to be ignored. Indeed, this assumption is so common in the open literature that both of these terms will be neglected in the remainder of this chapter.

The following sections of this chapter provide a description of the principal pdf modeling approaches discussed in the open literature for TRI closure. It is not the objective of this report to provide a detailed review of reaction and mixture models however. The interested reader is directed to, for example, Smoot and Smith (1985), Smith and Fletcher (1988), Puri (1993), Young and Moss (1995), DesJardin and Frankel (1998) for discussions of various models.

---

1. Personal communication with Professor P.Smith of The University of Utah, 1998.

4.1 Assumed Probability Density Function Closure

The most common approach to TRI closure is to assume the shape of the probability density function P in Equation (4.1). Common choices include the beta function pdf described previously (cf. Equation (3.12)) as well as the clipped Gaussian and top hat distributions (Smoot and Smith, 1985, pg. 278). The domain of each of these functions may be mapped onto the interval [0, 1] (a Gaussian distribution by contrast is nonzero on the interval $(-\infty, \infty)$). For example, Puri (1993) describes a beta pdf function based on mixture fraction[1] and the Favre mean and variance of the mixture fraction

$$P(f;\tilde{f},\tilde{f''^2}) = Cf^{a-1}(1-f)^{b-1}, \tag{4.2}$$

$$C = \left[\int_0^1 f^{a-1}(1-f)^{b-1}df\right]^{-1}, \tag{4.2a}$$

$$a = \frac{\tilde{f}^2(1-\tilde{f})}{\tilde{f''^2}} - \tilde{f}, \tag{4.2b}$$

$$b = \frac{\tilde{f}(1-\tilde{f})^2}{\tilde{f''^2}} - 1 + \tilde{f}. \tag{4.2c}$$

where f= 0 indicates pure oxidizer and f= 1 indicates pure fuel. Conservation equations for the Favre mean and variance, $\tilde{f''^2}$, of the mixture fraction are solved in Puri's model to provide a unique pdf shape at each point in the fire.

A reaction model is then required to complete the formulation by relating the absorptivity and temperature to the mixture fraction. For example, Hall and Vranos (1994, 1995) employ an opposed jet flame solution to obtain a state relationship between the temperature and species concentration and the mixture fraction. Since the absorptivity may in turn be expressed in terms of the species concentration, Equation (4.1) may be written

$$\overline{\mu_a e_b} = \int_0^1 \mu_a(f)e_b(f)P(f;\tilde{f},\tilde{f''^2})df. \tag{4.3}$$

For many applications of engineering interest, however, it is not possible to obtain such a simple reaction model for the absorptivity and temperature in terms of a single mixture variable. Strictly

1. For applications involving a single fuel and a single oxidizer stream, the mixture fraction at a given location represents the fraction of the mass which originated in the fuel stream.

speaking, Equation (4.3) is not valid for participating media and also assumes no flow work and unity Schmidt and Prandtl numbers. Nevertheless, the Hall and Vranos formulation is an example of a simple reaction model.

In contrast to the Hall and Vranos (1994, 1995) reaction model, Adams and Smith (1994, 1995) propose a reaction model based on the local stoichiometry, ϕ, and the enthalpy

$$\overline{\mu_a e_b} = \iint \mu_a(\phi, h) e_b(\phi, h) P_{\phi h}(\phi, h; \tilde{\phi}, \widetilde{\phi''^2}, \tilde{h}, \widetilde{h''^2}) d\phi dh . \tag{4.4}$$

In the formulation of Adams and Smith, fluctuations in the local enthalpy and stoichiometry are assumed to be statistically independent thus (Smoot and Smith, 1985, pg. 333)

$$P(\phi, h; \tilde{\phi}, \widetilde{\phi''^2}, \tilde{h}, \widetilde{h''^2}) = P_{\phi}(\phi; \tilde{\phi}, \widetilde{\phi''^2}) P_h(h; \tilde{h}, \widetilde{h''^2}) . \tag{4.5}$$

Similarly, Hartick, et al. (1995, 1996) also assume statistical independence for their reaction model based on mixture fraction and heat release rate and represent the joint pdf as the product of two beta pdfs. Although the assumption of statistical independence may not be strictly accurate, it is a common assumption which allows for the construction of the joint pdf from simpler forms. Given the insensitivity of the resulting mean to the shape of the pdf suggested by Table 3.2 it may be reasonable to expect that the assumption of statistical independence will only have a secondary effect on the resulting solution.

4.1.1 Eddy Dissipation Combustion Model

Magnussen's Eddy Dissipation Combustion (EDC) concept (Gran and Magnussen, 1996) is of particular interest in this report as a reaction/mixing model because the EDC model currently provides the TRI closure for the first generation fire simulation code under development in the Engineering Sciences Center at Sandia National Laboratories (Cochran et al., 1998). It may also not be immediately apparent that the EDC model can be described using the pdf formalism described above.

Using the form of Equation (4.1) the mean radiative source term, assuming gray transport, for the EDC reaction/mixing model is given by

$$\overline{\mu_a e_b} = \overline{\mu_a}(\overline{X_i}, \overline{T}) \int_T T^4 P(T; \overline{X_i}, \overline{h}, k, \varepsilon) dT , \tag{4.6}$$

where X_i are species concentrations, k is the turbulent kinetic energy, and ε is the turbulent dissipation rate. The EDC model also assumes gray radiative transport as implied by the T^4 term in Equation (4.6). As suggested by Equation (4.1), the shape of the pdf in the EDC mixing model should be dictated by the mean temperature and the moments of the temperature fluctuations. This dependence is implied in Equation (4.6) since the mean enthalpy and species concentrations (with the specific heats) provide the mean temperature and the turbulent kinetic energy and

dissipation rate provide information regarding the turbulent temperature fluctuations. This will be described in greater detail below and is fully described in Cochran et al., (1998). An important aspect of the EDC reaction/mixing model is that, by using the mean absorption coefficient, *the model neglects the absorptivity-temperature correlation effect.*

The EDC mixing model which dictates the form of the pdf function may be described as a two zone model comprising a flame zone and a surrounding zone. Without providing the details of the development (see Cochran et al., 1998), the temperatures of the flame zone and the surrounding zone are functions of the mean enthalpy and the mean species concentrations. The volume fraction of the flame zone and surroundings are then given by the turbulent kinetic energy and dissipation rate. With these values, the shape of the pdf in Equation (4.6) is given by the double Dirac function shown in Figure 4.1. As mentioned above, the variance of the temperature may be calculated from the flame and surroundings temperature and the flame volume fraction.

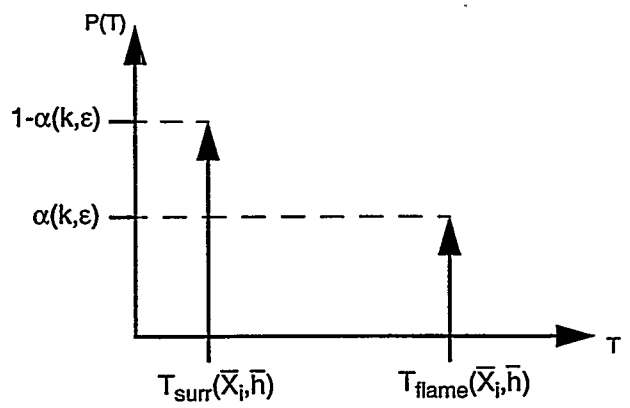

FIGURE 4.1 - Probability density function for the eddy dissipation combustion concept mixing model.

The variation of the temperature self correlation term with temperature fluctuation intensity may be evaluated using the EDC model for the particular case of α=0.1 as shown in Figure 4.2. For comparison, Figure 4.2 also shows the temperature self correlation predicted by the beta PDF shown previously in Figure 3.1. Although the EDC model prediction for the temperature self correlation is slightly higher than that predicted by the beta PDF, all three curves are remarkably close given the differences in the overall PDF shapes. As with Figure 3.1 the data in Figure 4.2 suggests that the particular shape of the PDF is not as important as the details of the mixing and reaction models which provide, in the case of the EDC model, T_{surr}, T_{flame}, and α.

4.2 Direct Probability Density Function Closure

Another approach to turbulence radiation interaction closure modeling is the direct probability density function approach described by Mazumder and Modest (1997a). The details of this formulation are reasonably involved (Pope, 1985, Pope, 1990, Mazumder, 1997, Mazumder and Modest, 1997b, Mazumber and Modest, 1997c) and, for the purposes of this report, not extremely illuminating. Therefore, the direct pdf approach will only be described in words here with specific references made to modeling issues of importance to TRI closure.

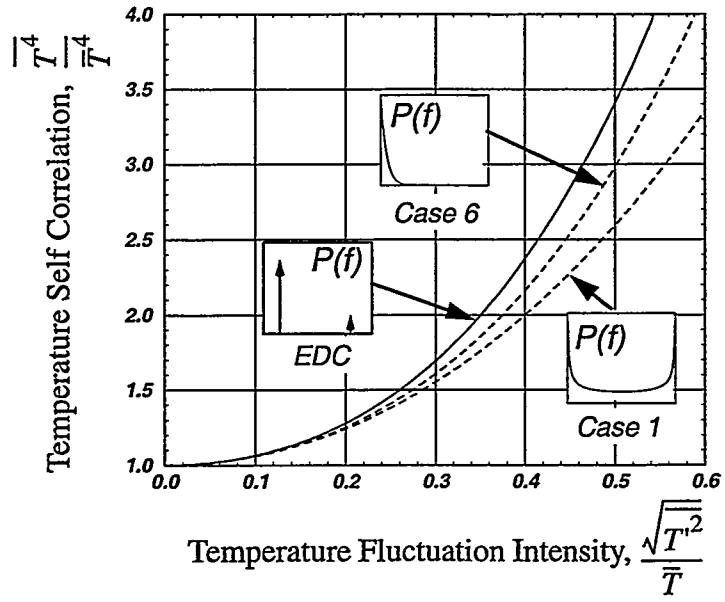

FIGURE 4.2 - Temperature self correlation variation with temperature fluctuation intensity for the Eddy Dissipation Combustion (EDC) model compared to limiting cases using beta probability density functions

In general terms, the direct pdf method does not assume the shape of the pdf but rather the shape, " ... is calculated from a modelled evolution equation for the pdf." (Pope, 1985, pg. 121). In the direct pdf method, this is accomplished by representing the fluid as a large number of notional particles each having a unique position, velocity, temperature, and species concentration. Each of these particles is governed by a set of Lagrangian transport equations for the particle velocity, temperature, and species concentration (Mazumder, 1997, Mazumder and Modest 1997a).

The formulation described by Mazumder and Modest (1997a) employs a coupled finite volume solution for the radiative transport on a structured grid and a Lagrangian solution for the particle temperature, velocity, and species concentration. During the radiation solution, the absorptivity-temperature correlation term for a given volume is calculated from

$$\overline{\mu_a' e_b'} \approx \frac{1}{N_p} \sum_{i=1}^{N_p} (\mu_{a,i} - \langle \mu_a \rangle)(e_{b,i} - \langle e_b \rangle), \tag{4.7}$$

where the brackets $\langle\ \rangle$ indicate an ensemble average over all of the particles in the volume. The use of the term "direct pdf method" becomes more apparent in Equation (4.7) since the integration shown in Equation (4.1) is carried out implicitly by the distribution of the particle values and, mechanically, the integration becomes a simple sum over the particles in a cell.

One of the attractive aspects of the direct pdf method described by Mazumder and Modest (1997a) is that this formulation does not treat turbulence as a simple random process but

recognizes the origins of turbulent instabilities in the governing transport equation. Nevertheless, the direct pdf method still requires turbulent closure models and near wall treatments (Mazumder and Modest, 1997b) within the Lagrangian transport equations. These closure models are based on various stochastic processes, e.g., Poisson process, Markovian process, etc., which must be combined appropriately to accurately represent the turbulent fluctuations for a given application (Mazumder, 1997). It is not clear that these implementation challenges for the Lagrangian turbulent closure models are any less significant than their Eulerian counterparts.

Another important aspect of the direct pdf method is that the Lagrangian transport equations involve spatial gradients of the mean flow properties. This requires some form of spatial averaging of the particle values to obtain these mean gradients. Pope (1985) indicates that ensemble averages over cells to obtain these derivatives is, " ... hopelessly inaccurate ... " and the use of least squares cubic splines is recommended. Coupling of the direct pdf method to a grid based solution for the radiative transport may also require that the cells used for spatial averaging coincide with those used for the radiative transport which may be problematic for unstructured grids.

One method for resolving this spatial averaging difficulty may be in coupling the direct pdf method to a conventional Eulerian solution for the mean flow[1]. In this case the Lagrangian particles would be used only to provide closure for the turbulent correlation terms in the mean equations. It is also possible that such an approach may not require as many particles as would be required to describe the mean flow as well.

The Monte Carlo nature of the direct pdf method also raises concerns for its parallel implementation using a spatially decomposed geometry on a distributed memory machine. Spatial decomposition is a common parallel decomposition paradigm for many parallel computational fluid mechanics applications and is often required for even moderately complex geometry. The communication of particles between processors in such an application gives rise to a highly asynchronous communication pattern which is difficult to optimize for unstructured grids.

4.3 Summary

In this chapter the assumed EDC and direct pdf TRI closure models have been summarized. These models represent the two principal TRI closure models described in the open literature. Each of these models provide closure only for the absorptivity-temperature correlation and temperature self correlation terms. The thin eddy approximation is commonly employed throughout the open literature and allows the absorptivity-intensity and absorptivity-scalar flux correlations to be ignored.

The assumed pdf method provides a general framework in which a number of turbulent reaction and mixing models may be implemented. In general, the assumed pdf method involves the specification of a transport equation for the mean and variance of each of the reaction and mixing variables used to describe the particular turbulent reaction and mixing models. An assumed

1. Personal communication with Professor Michael Modest of The Pennsylvania State University, 1998.

functional form is then developed using the mean and variance of the reaction and mixing variables to provide the pdf function for the turbulent fluctuations in the flow properties at each point in the computational domain. The EDC reaction/mixing model represents one example of an assumed pdf model which involves a single reaction variable and which ignores the absorptivity-temperature correlation term and treats only the temperature self correlation term.

The direct pdf method employs a Lagrangian description to provide turbulence closure using ensemble averages over a number of particles which represent the flow. While the direct pdf is relatively intuitive, it still requires turbulence closure models which are perhaps no less challenging than standard Eulerian closure models. The Monte Carlo nature of the direct pdf method also raises concern for parallel implementation using spatial decomposition on a distributed memory machine. A number of alternatives may be available to circumvent these difficulties and the direct pdf method has other attractive characteristics which warrant continued research to obtain an optimum implementation.

5.0 CONCLUSIONS

The following list summarizes the principal observations made in this review.

1) Turbulence radiation interaction (TRI) is an important consideration for turbulent reacting flow problems. This is confirmed by experimental evidence and simple numerical results both of which show that the radiative heat flux and radiative source term in a turbulent flame may be 2-3 times larger than estimates based on the mean temperature and absorptivity.

2) The TRI closure problem for the time averaged conservation and Boltzmann equations is comprised of four principal terms: the absorptivity-intensity correlation, the absorptivity-scalar flux correlation, the temperature self correlation, and the absorptivity-temperature correlation.

3) A common approximation for turbulent flames in which the optical thickness of the turbulent eddies is small is to neglect the absorptivity-intensity correlation. The rationale for this approximation is that, under these conditions, the local intensity is a function of the temperature and material properties extending over several mean free paths and, as a result, it is weakly correlated with the local absorptivity.

4) Similar arguments may be made for neglecting the absorptivity-scalar flux correlation under conditions of optically thin turbulent eddies.

5) The nonlinear dependence of the Planck function on the temperature gives rise to a significant temperature self correlation effect. Simple numerical experiments show that, given experimentally observed turbulent temperature fluctuation intensities, the temperature self correlation term can easily account for a 100% increase in the emissivity of a turbulent flame relative to the mean temperature.

6) Some experimental and numerical evidence suggests that the absorptivity-temperature correlation effect may be small relative to the temperature self correlation effect for heavily sooting flames. This absorptivity-temperature correlation effect is difficult to measure in general and its magnitude relative to the temperature self correlation effect is open to conjecture.

7) Three principal modeling approaches may be identified in the open literature to provide TRI closure: the more common assumed pdf method, the EDC model, which has been shown to be a simple pdf method, and the direct pdf method. In each of these models the thin eddy approximation is commonly employed allowing the absorptivity-intensity and absorptivity-scalar flux correlation terms to be ignored.

8) The assumed pdf method describes a general framework in which a number of turbulent reaction and mixing models may be implemented.

9) The eddy dissipation combustion (EDC) reaction/mixing model is an example of a simple assumed pdf turbulent mixing/reaction model. The EDC model ignores the absorptivity-temperature correlation and considers only the temperature self correlation.

10) The direct pdf method employs a Lagrangian description of a large number of fluid particles to provide closure for the turbulent fluctuating correlations. While the direct pdf has been used for TRI closure, it is not as widely used as the assumed pdf method and a continued research is needed to provide an optimum implementation.

APPENDIX A KOLMOGOROV LENGTH SCALE ESTIMATE

The Kolmogorov length scale for the smallest turbulent eddies is given by Tennekes and Lumley (1972, pg. 20) to be

$$\kappa = \left(\frac{\nu^3}{\varepsilon}\right)^{1/4}, \tag{A.1}$$

where ν is the kinematic viscosity, κ is the Kolmogorov length scale of the smallest turbulent eddies, and ε is the turbulent dissipation rate. The dissipation rate may then be expressed in terms of the characteristic velocity fluctuation, u, and the integral scale of the largest turbulent eddies, δ

$$\varepsilon = \frac{u^3}{\delta}. \tag{A.2}$$

For a buoyant plume, the integral scale, δ, is approximately the radius of the plume and the velocity fluctuation is on the same order as the mean flow (Tennekes and Lumley, pg. 137). Thus, Equation (A.1) reduces to

$$\kappa = \left(\frac{L_o \nu^3}{2v_o^3}\right)^{1/4}. \tag{A.3}$$

Substituting the scale values from Table 1.1 into Equation (A.3) ($\nu \approx 10^{-5}$ m^2/s) results in an order of magnitude estimate for the Kolmogorov length scale for a large scale hydrocarbon pool fire of $O(10^{-5})$ to $O(10^{-4})$ m.

REFERNCES

ADAMS, B.R., SMITH, P.J., 1995, "Modeling Effects of Soot and Turbulence-Radiation Coupling on Radiative Transfer in Turbulent Gaseous Combustion," *Combustion Science and Technology*, 109:121-140

ADAMS, B.R., SMITH, P.J., 1994, "Modeling Effects of Soot and Turbulence-Radiation Coupling on Radiative Transfer in an Industrial Furnace", *Proceedings of the Sixth AIAA/ ASME Thermophysics and Heat Transfer Conference, Radiative Heat Transfer: Current Research*, HTD-vol. 276, pp. 177-190

BEJAN, A., 1991, "Predicting the Pool Fire Vortex Shedding Frequency," *Journal of Heat Transfer*, 113:261-263

COPPALLE, A., JOYEUX, D., 1994, "Temperature and Soot Volume Fraction in Turbulent Diffusion Flames: Measurements of Mean and Fluctuating Values," *Combustion and Flame*, 96:275-285

COCHRAN, R.J., MARTINEZ, M.J., EVANS, G.H., BLOTTNER, F.G., BURNS, S.P., TIESZEN, S.R., MOEN, C.D., NICOLETTE, V.F., GRITZO, L.A., 1998, *SIERRA/Fuego Theory Manual*, Sandia National Laboratories Technical Report, Sandia National Laboratories, Albuquerque, NM (to be published)

COX, G., 1977, "On Radiant Heat Transfer in Turbulent Flames", *Combustion Science and Technology*, 17:75-78

DESJARDIN, P.E., FRANKEL, S.H., 1998, "Large Eddy Simulation of a Nonpremixed Reacting Jet: Application and Assessment of Subgrid-Scale Combustion Models," *Physics of Fluids*, 10(9)1-17

FAETH, G.M., JENG, S.M., GORE, J., 1985, "Radiation from Fires", *Heat Transfer in Fire and Combustion Systems*, C.K. Lau, Y. Jaluria, W.W. Yuen, K. Miyasaka eds., ASME, New York, pp. 137-151

GORE, J.P., FAETH, G.M., 1986, "Structure and Spectral Radiation Properties of Turbulent Ethylene/Air Diffusion Flames," *Proceedings of the Twenty-First Symposium (International) on Combustion*, pp. 1521-1531

GORE, J.P., FAETH, G.M., 1988, "Structure and Radiation Properties of Luminous Turbulent Acetylene/Air Diffusion Flames," *Journal of Heat Transfer*, 110:173-181

GORE, J.P., JENG, S.M., FAETH, G.M., 1987, "Spectral and Total Radiation Properties of Turbulent Hydrogen/Air Diffusion Flames," *Journal of Heat Transfer*, 109:165-171

GORE, J.P., IP, U.S., SIVATHANU, Y.R., "Coupled Structure and Radiation Analysis of Acetylene/Air Flames," *Journal of Heat Transfer*, 114:487-493

GRAN, I., MAGNUSSEN, B.F., 1996, "A Numerical Study of a Bluff-Body Stablized Diffusion Flame. Part 2 - Influence of Combustion Modeling and Finite Rate Chemistry," *Combustion Science and Technology*, 119:191-217

GRITZO, L.A., SIVATHANU, Y.R., GILL, W., 1998, "Transient Measurements of Radiative Properties, Soot Volume Fraction and Soot Temperature in a Large Pool Fire," Accepted to *Combustion Science and Technology*

HALL, R.J., VRANOS, A., 1994, "Efficient Calculations of Gas Radiation from Turbulent Flames", *International Journal of Heat and Mass Transfer*, 37(17):2745-2750

HALL, R.J., VRANOS, A., 1995, "Incorporation of an Efficient Turbulent Radiation Algorithm into a Discrete Transfer Program," *Heat and Technology - Calore e Tecnologia*, 13(2):155-168

HARTICK, J.W., NEUBER, A.A., FRUCHTEL, G., HASSEL, E.P., JANICKA, J., 1995, "Turbulence-Radiation Interaction in Confined Combustion Systems," *Forschung im Ingenieurwesen-Engineering Research*, 61(3):67-74

HARTICK, J.W., TACKE, M., FRÜCHTEL, G., HASSEL, E.P., JANICKA, J., 1996, "Interaction of Turbulence and Radiation in Confined Diffusion Flames", *Proceedings of the Twenty-Sixth Symposium (International) on Combustion*, pp. 75-82

KABASHNIKOV, V.P., KMIT, G.I., 1979, "Influence of Turbulent Fluctuations on Thermal Radiation", *Journal Applied Spectroscopy*, 31(2):963-967

KABASHNIKOV, V.P., MYASNIKOVA, G.I., 1985, "Thermal Radiation in Turbulent Flows - Temperature and Concentration Fluctuations", *Heat Transfer - Soviet Research*, 17(6):116-125

KOUNALAKIS, M.E., GORE, J.P., FAETH, G.M., 1988, "Turbulence/Radiation Interactions in Nonpremixed Hydrogen/Air Flames," *Proceedings of the Twenty-Second Symposium (International) on Combustion*, pp. 1281-1290

KOUNALAKIS, M.E., SIVATHANU, Y.R., FAETH, G.M., 1991, "Infrared Radiation Statistics of Nonluminous Turbulent Diffusion Flames," *Proceedings of the Joint ASME/JSME Thermal Engineering Conference*, 5:3-12

KÖYLÜ, Ü.Ö., FAETH, G.M., 1992, "Structures of Overfire Soot in Buoyant Turbulent Diffusion Flames at Long Residence Times," *Combustion and Flame*, 89:140-156

KÖYLÜ, Ü.Ö., FAETH, G.M., 1996, "Spectral Extinction Coefficients of Soot Aggregates from Turbulent Diffusion Flames," *ASME Journal of Heat Transfer*, 118(2):415-421

KREBS, W., KOCH, R., GANZ, B., EIGENMANN, L., WITTIG, S., 1996, "Effect of Temperature and Concentration Fluctuations on Radiative Heat Transfer in Turbulent

Flames", *Proceedings of the Twenty-Sixth Symposium (International) on Combustion*, pp. 2763-2770

MAZUMDER, S., 1997, "Numerical Study of Chemically Reactive Turbulent Flows with Radiative Heat Transfer," *Ph.D. Dissertation*, The Pennsylvania State University

MAZUMDER, S., MODEST, M.F., 1997a, "PDF Modeling of Turbulence-Radiation Interactions," *Volume 7 of the Proceedings of the 32nd ASME National Heat Transfer Conference, HTD-Vol. 345*, Baltimore, Maryland, 1-12

MAZUMDER, S., MODEST, M.F., 1997b, "Boundary Treatment and an Efficient Pressure Algorithm for Internal Turbulent Flows Using the PDF Method," *International Journal for Numerical Methods in Fluids*, 24(2):215-232

MAZUMDER, S., MODEST, M.F., 1997c, "A Stochastic Lagrangian Model for Near-Wall Turbulent Heat Transfer," *Journal of Heat Transfer*, 119(1):46-52

MODEST, M.F., 1993, *Radiative Heat Transfer*, McGraw-Hill, Inc., New York, NY

NELSON, D.A., 1989a, "Band Radiation from a Nonhomogeneous Fluctuating Medium", *Heat Transfer Phenomena in Radiation, Combustion, and Fires*, R.K.Shah ed., HTD-vol. 106, ASME, New York, pp. 287-293

NELSON, D.A., 1989b, "Band Radiation from a Fluctuating Medium", *Journal of Heat Transfer*, 111:131-134

POPE, S.B., 1985, "PDF Methods for Turbulent Reactive Flows," *Progress in Energy and Combustion Science*, 11(2):119-192

POPE, S.B., 1990, "Computations of Turbulent Combustion: Progress and Challenges," *Twenty-Third Symposium(International) on Combustion*, Orleans, France, The Combustion Institute, Pittsburg, Pennsylvania, 561-612

PURI, I.K., 1993, *Environmental Implications of Combustion Processes*, CRC Press, Boca Raton, FL

SIEGEL, R. , HOWELL, J.R., 1992, *Thermal Radiation Heat Transfer, Third Edition*, Hemisphere Publishing Corp., Washington, DC

SIVATHANU, G.M., KOUNALAKIS, M.E., FAETH, G.M., 1990, "Soot and Continuous Radiation Statistics of Luminous Turbulent Diffusion Flames," *Proceedings of the Twenty-Third Symposium (International) on Combustion*, pp. 1543-1550

SMITH, P.J., FLETCHER, T.J., 1988, "A study of Two Chemical Reaction Models in Turbulent Coal Combustion," *Combustion Science and Technology*, 58:59-76

SMOOT, L.D., SMITH, P.J., 1985, *Coal Combustion and Gasification*, Plenum, New York

SOUFIANI, A., MIGNON, P., TAINE, J., 1990, "Radiation-Turbulence Interaction in Channel Flows of Infrared Active Gases," *Proceedings of the International Heat Transfer Conference*, 6:403-408

TENNEKES, H., LUMLEY, J.L., 1972, *A First Course in Turbulence*, The MIT Press, Cambridge, Massachusetts

WILCOX, D.C., 1998, *Turbulence Modeling for CFD, Second Edition,* DCW Industries, Inc., La Canada, CA

YOUNG, K.J., MOSS, J.B., 1995, "Modelling Sooting Turbulent Jet Flames Using and Extended Flamelet Technique," *Combustion Science and Technology*, 105:33-53

Distribution

1	MS 9042	W.G.Houf
1	MS 0828	T.C.Bickel
1	MS 0835	R.J.Cochran
20	MS 0835	S.P.Burns
1	MS 0836	P.E.DesJardin
1	MS 0836	L.A.Gritzo
1	MS 0836	C.W.Peterson
1	MS 0836	S.R.Tieszen
1	MS 1111	R.C.Schmidt
1	MS 1111	J.N.Shadid
1	MS 0835	S.N. Kempka
1	MS9018	Central Technical Files, 8940-2
2	MS 0899	Technical Library, 4916
1	MS 0612	Review and Approval Desk, 4912 For DOE/OSTI

1 Dr. Jayavant P. Gore
College of Engineering
Purdue University
1003 Chaffee Hall
West Lafayette, IN 47907-1003

1 Dr. John R. Howell
Associate Dean
College of Engineering
The University of Texas at Austin
ECJ 10.338
Austin, TX 78712

1 Dr. Michael Modest
College of Engineering
The Pennsylvania State University
0301C Reber Building
University Park, PA 16802

1 Dr. Philip Smith
College of Engineering
University of Utah
3290 MEB
Salt Lake City, UT 84112-1180

1 Dr. Bjorn Magnussen
Department of Applied Thermodynamics
Norwegian Institute of Science
and Technology
Kolbjorn Hejes Vei 1B
Trondheim, Norway
N-7034